Vibration Troubleshooting of an Air Compressor

William D. Marscher and **James J. McGinley**, Mechanical Solutions, Inc., Whippany, New Jersey

An experimental investigation was conducted to determine the cause of cyclic vibration of a double overhung air compressor. The problem was solved by increasing the inlet temperature of oil to the bearings.

Vibration troubleshooting is described for a double overhung air separation compressor that was exhibiting slow (order of minutes) but dramatic oscillations at 1× running speed, in gross violation of ISO and military specifications. The compressor ran for years without vibration problems. Recently, modifications were made to the oil supply system allowing for additional passive cooling on hot days. The temperature decrease resulted in high cyclic vibration levels, cycling in a sinusoidal motion over a period of several minutes whenever the bearing supply temperature dropped below 125° F.

None of the common causes of excess 1× vibrations, operating alone, should cause the cyclic behavior observed. Shaft bow, however, has been observed by others in certain cases to alter bearing energy dissipation and promote thermally-induced kinking of the shaft in a cyclic manner through a phenomenon known as the Morton Effect. A thermal gradient develops across the shaft within a journal bearing, due to viscous shearing forces on the consistently loaded side of the bearing film during synchronous (1× running speed) whirl. Heat dissipation at the close clearance causes this side of the shaft to expand more than the other side, and results in thermally-induced shaft bow. As this thermal bow accumulates, the shaft experiences additional effective unbalance that tends to counter any original shaft bow or imbalance, unloading the bearing. This moves the hot spot in a manner that moves gradually around the shaft, eventually returning to its original spot, causing cycling. In a double overhung rotor such as the one involved here, this effect was found to happen with peak cycle amplitude at each end occurring at different times, and with the apparent phase angle shift of the "hot spot" being limited in a deceiving, but explainable, manner.

Field testing showed that maintaining an oil inlet temperature above a practical threshold temperature minimized viscous shearing forces in the bearing film enough to prevent the thermal cycling from occurring. Another option for eliminating the problem would be a bearing re-design to reduce hot spot temperature severity.

Testing Procedures

Various vibration probes were installed to observe the compressor stages during steady operation, both when the oil temperatures were high, as well as when they were at their minimum. The temperature of the oil was monitored throughout the testing process. A 14-channel B&K Pulse FFT spectrum analyzer and digital tape recorder was used for the testing. Vibration instrumentation consisted of piezoelectric miniature accelerometers mounted in three orthogonal directions on the bearing housings, and eddy current proximity probes mounted immediately next to each bearing in two orthogonal radial directions. Vibration frequency spectra were documented, as well as vibration amplitude versus time, phase angle (versus a keyphasor reference) versus time, and shaft orbits at each of the two bearings for the problem shaft. Plant DCS thermistors, calibrated to ±0.5° F, were used to determine bearing inlet oil temperature.

Results and Discussion

MSI (Mechanical Solutions, Inc.) confirmed that the vibration spectra did not show any evidence of significant subsynchronous (below running speed) vibration, or of a resonance. Impact testing with a calibrated hammer was used during operation using the authors' Time-Averaged Pulse technique to determine the frequency and damping of each rotor and structural natural frequency near running speed, and within the range of zero to blade passing frequency. Results were confirmed by logarithmic plotting of the natural excitation frequency response spectra, which exhibited an absence of broadband resonant peaks near any significant narrowband excitation forcing frequencies. In addition, in the logarithmic spectra, there was no evidence of excessive or unexpected aerodynamic forces, such as rotating stall, which typically show up in the spectrum also as relatively broad peaks, at frequencies associated with the average rotation of static pressure or velocity fields.

Figures 1-3 show the orbits and logarithmic frequency spectra of the two compressor stages (single stage overhung wheels, on opposite sides of the same rotor, with two intervening load-between-pads tilting pad bearings), with vibration in mils. Figure 1 shows the left bearing orbit over one full cycle. Figure 1A shows the orbit near the peak of the cycle. Over time the orbit starts to decrease, shown in Figures 1B and 1C. In Figure 1D the orbit has reached its minimum level in the cycle. The orbit then begins to increase (Figures 1E-G) until it reaches its maximum value, shown in Figure 1G. Figure 1H shows the orbit at the same location in the cycle as Figure 1A.

Figures 2 and 3 show the proximity probe vibration spectra from both bearings during the cycling. Both spectra are plotted with a logarithmic scale in order to emphasize the broadband vibration content. The narrow band vibration peaks at 255 Hz, represent the 1× running speed vibration level. These synchronous vibration peaks contain the majority of the overall vibration content in the spectra. A broadband 'mountain' peak can be seen near 195 Hz. This broadband peak represents the first bending mode of the rotor and is sufficiently below running speed to avoid resonance.

Vibration measured with accelerometers on the stationary casing of the machine was relatively low and did not participate significantly in the problem vibration levels of the rotors. Therefore, accelerometer data were not plotted.

Figure 4 compares plots of the peak amplitude of the shaft vibration envelope versus time, as well as phase angle versus the keyphasor reference location. These plots clearly show the cycling between ends of the rotor. The presence of the phase cycling is important since it indicates that the net vector force acting on the rotor must be changing its phase angle with respect to the rotor clock position. The magnitude and phase information contained in Figure 4 was converted into a polar plot (Nyquist Plot, Figure 5), where the magnitude is the radial length from the origin and the phase is the angle from the positive X-axis to the vector. Plotting the data in this form allowed assessment of the magnitude and phase information from one data point at a time.

The authors concluded that the gradual cycling of the synchronous vibration has been caused by the Morton Effect, as discussed in References 1-4. The Morton Effect is a synchro-

Based on a paper which was presented at the Society for Machinery Failure Prevention Technology Annual Conference, Virginia Beach, VA, April 2004.

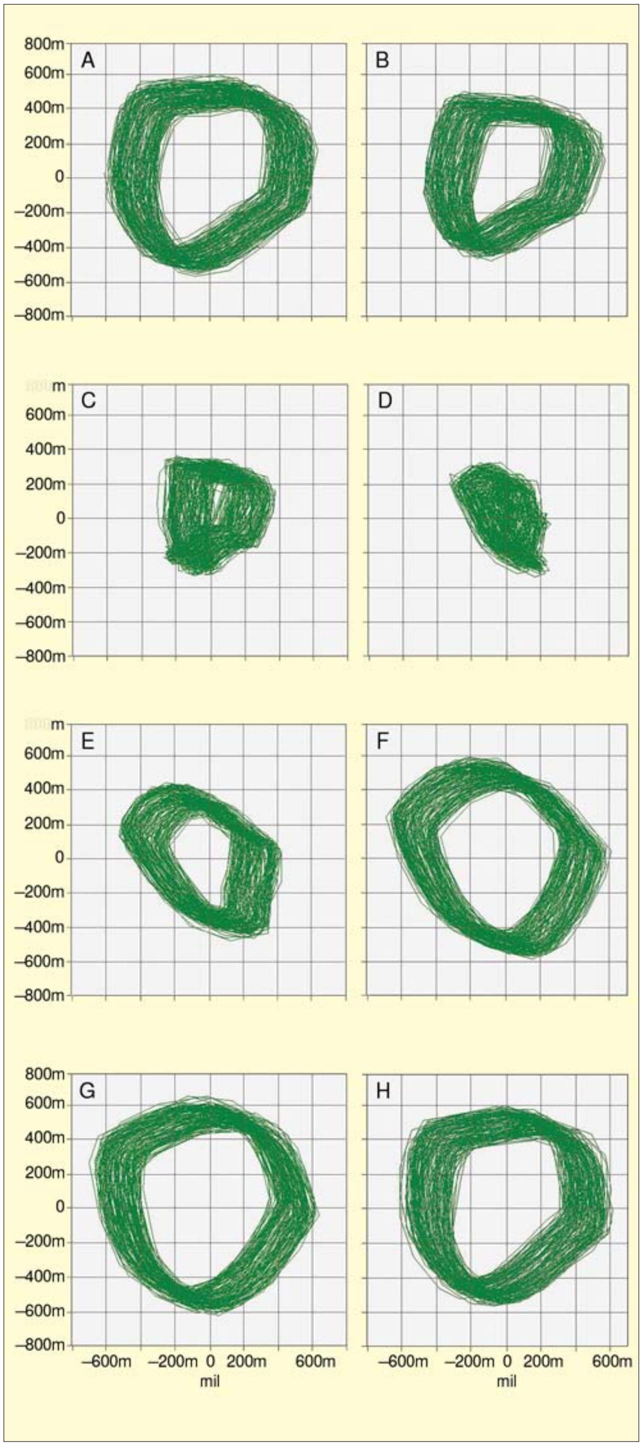

Figure 1. A – Left bearing orbit (near peak amplitude), 0 sec into test. B – Left bearing orbit at 45 sec into test. C – Left bearing orbit at 90 sec into test. D – Left bearing orbit at 135 sec into test. E – Left bearing orbit at 180 sec into test. F – Left bearing orbit at 225 sec into test. G – Left bearing orbit at 315 sec into test. H – Left bearing orbit at 360 sec into test.

nous vibration phenomena that results from a thermal gradient imposed on the shaft within the bearing during operation, typically by close-clearance viscous shear at the same spot on a shaft journal as it whirls synchronously. The thermal growth due to the thermal gradient creates a bow in the shaft that results in thermally-induced imbalance. When such a thermal gradient is caused by viscous forces in the bearings, as oil temperature is decreased, viscous shearing forces increase, causing increased bow, to the point that induced bow may compete with the original mechanical imbalance and/or residual bow. In the case of the tested rotor, once the oil temperature dropped below approximately 125° F, the thermal imbalance became

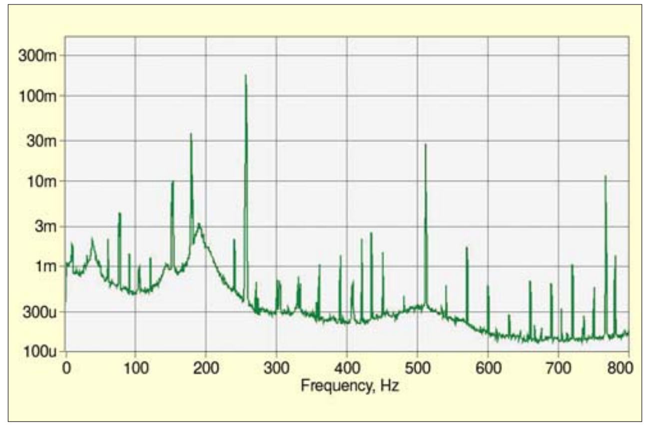

Figure 2. Vibration spectrum of left bearing proximity probe (100 linear averages). Note – running speed is 255 Hz.

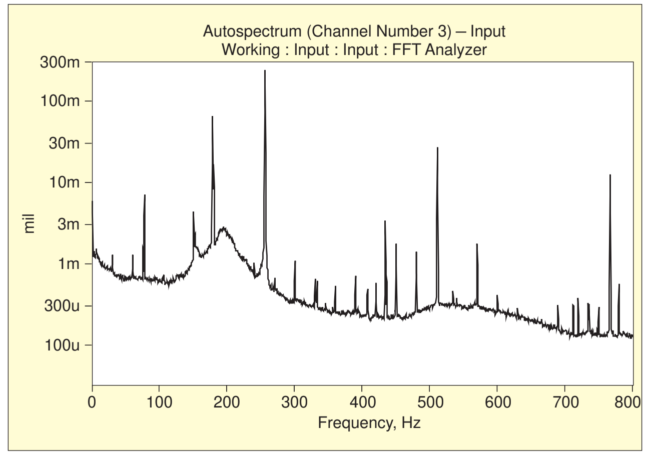

Figure 3. Vibration spectrum of right bearing proximity probe (100 linear averages). Note – running speed is 255 Hz.

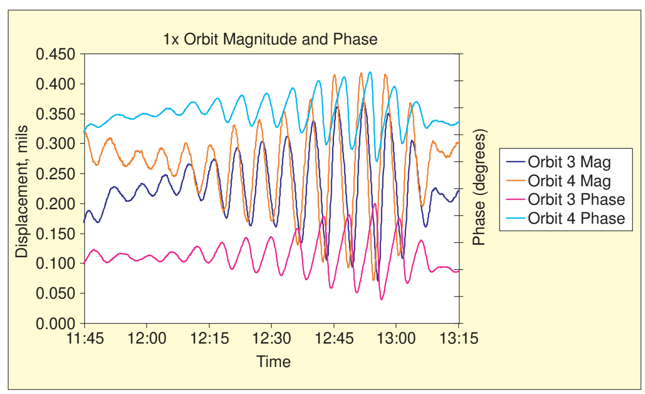

Figure 4. Synchronous vibration levels of bearings vs. time (hr:min).

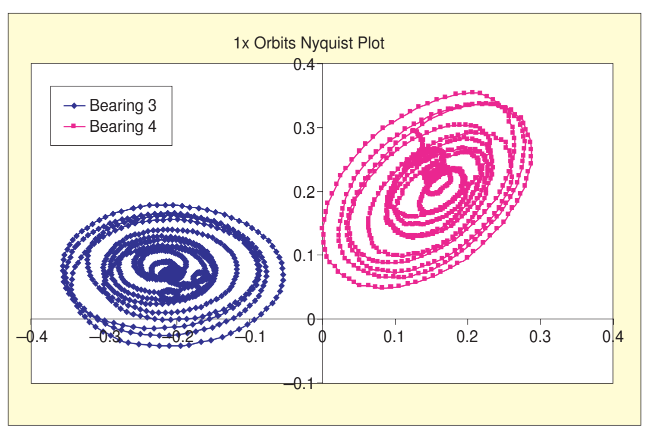

Figure 5. Nyquist plots of left ("Bearing 3") and right ("Bearing 4") orbits.

large enough to compete with the residual mechanical imbalance in this manner, thereby changing the angular location of heat input, the direction and amount of the net bow, and therefore the level and phasing of peak vibration response, initiating vibration amplitude cycling.

The Nyquist plot in Figure 5 shows the consistent cycling of the magnitude and phase of the two bearing orbits. The magnitude and phase of the orbits cycled in a manner suggesting that the overall cyclic vector force on the rotor acted over a full 360° through one complete cycle. Figure 6 shows the residual mechanical imbalance vectors and the apparent cyclic thermal imbalance (resulting from the thermal shaft bow) vectors overlaid on the Nyquist plot. This experimental plot clearly shows that the cyclic thermal vectors must act over a full 360° during one complete cycle. The Nyquist plot shows, however, that the net global phase angle change taken up by the two orbits is deceptively only ~60°, misleading previous troubleshooters to look for causes other than the Morton Effect.

Figure 7 shows the extreme net force vectors for the two orbits and the phase angle between them. The location of the temperature gradient will depend on the phase angle of the net force vector (i.e., the sum of the thermal and the mechanical imbalance vector). Therefore, the phase angle of the thermal imbalance will cycle with the phase angle of the net force vector. The test data show that the combined thermal imbalance from both ends must cycle 360° but that the individual net thermal plus mechanical imbalances only cycle approximately 60°. Synergistic cycling of the two ends is possible if the cycling can be resolved into vectors such that at least part of the thermal imbalances are 90° out of phase. This would be the general case and the locations of individual thermal imbalances would typically have a phase angle between them. It would be an unusual coincidence for both rotor ends to have their residual imbalance and/or bow in the same circumferential location.

At oil inlet temperatures above 128° F, the viscous shearing forces were small and did not create a large enough thermal imbalance to lead to cycling. Below 128° F, the shearing forces increased to the point that an oscillation threshold was reached, as predicted by Kirk et al,[4] and some degree of cycling was seen. As the temperature was further decreased, the thermal cycling increased in magnitude. Once the temperature was brought back above 128° F, the thermal cycling was observed to end and the vibration levels remained steady and moderate.

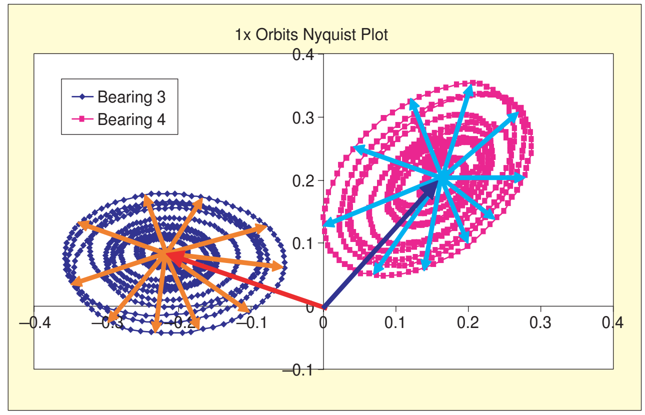

Figure 6. Nyquist plots of orbits with residual mechanical imbalance and cyclic thermal imbalance vectors overlaid.

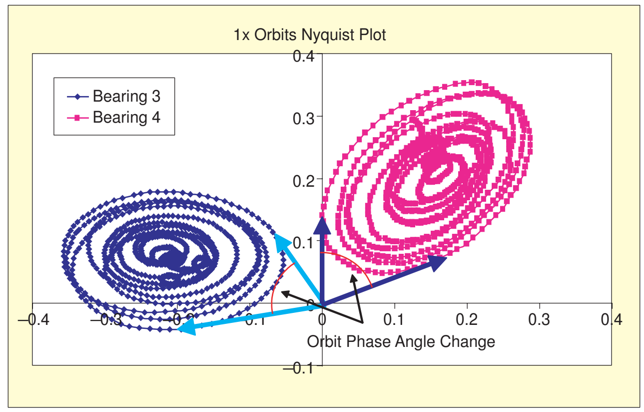

Figure 7. Nyquist plots of orbits 3 and 4 with net imbalance force vectors overlaid.

Conclusions

1. When oil inlet temperature was below a threshold level of 125° F, rotor vibration on the rotor was observed to cycle to excessive levels (over 1.2 mils p-p for this 15,300 rpm rotor) according to a consistent period of about 6 min. The left stage versus right stage ends cycled roughly 60° out of phase with each other. Increasing oil inlet temperature above 128° F effectively eliminated the high vibration and long cycling.
2. The vibration was nearly all at 1× running speed, typically symptomatic of resonance, imbalance, shaft bow or insufficient bearing stiffness.
3. There was no evidence of unstable subsynchronous or resonant 1× vibration. In the case of a rotordynamic instability, the vibration frequency would typically be in the range of 43-48% of running speed, which was not the case. In the case of resonant 1× vibration, typically a 'skirt' occurs at the bottom of the 1× vibration narrowband peak, and such a skirt was not present.
4. If the problem was due solely to an imbalance, it would not be expected to slowly cycle, and the vibration of each stage of the rotor would be expected to increase or decrease in phase, end-to-end, due to changing conditions of operation. In this case, slow oscillation occurred, in a manner that was not in phase end-to-end. The Newkirk Effect (rotor rubbing, heating, wearing, cooling and thereby reversing imbalance location on a cycling basis) could possibly explain this, but if so the rotor would have been expected to quickly wear itself out, which did not occur.
5. If the problem was insufficient bearing stiffness, then a large synchronous orbit would result, as was observed. Such low stiffness could be a flaw in bearing design or manufacture, for example by the clearance being too large. Typically, this would not lead to rotor vibration amplitude cycling.
6. If the problem was due to mechanical shaft bow, similar symptoms to imbalance would be anticipated. "Morton Effect" is a form of imbalance or bow which is cyclic. Depending on the phasing of the thermal unbalance and the mechanical unbalance of the two ends, a cyclic vibration pattern similar to the test data presented becomes possible.
7. The circular relationship of cyclic vibration amplitude with phase change at each end is best explained by the Morton Effect. Inlet oil temperature increase was effective in solving the problem, as was anticipated. A bearing design less prone to development of local hot spots would also be an effective solution.

References

1. De Jonge, F. M. and Morton, P. G., "The Synchronous Instability of a Compressor Rotor Due to Bearing Journal Differential Heating," ASME Paper 94-GT-35, pp. 1-13, 1994.
2. Keogh, P. S. and Morton, P. G., "The Dynamic Nature of Rotor Thermal Bending Due to Unsteady Lubricant Shearing Within Bearing," Proc. Royal Soc. of London, Series A, n. 445, pp. 273-290, 1994.
3. Faulkner, H. B., Strong, W. F. and Kirk, R. G., "Thermally Induced Synchronous Instability of a Radial Inflow Overhung Turbine," DETC97/VIB-4063, Proc. ASME Design Engineering Technical Conf, Sept. 14-17, 1997, Sacramento, CA, 1997.
4. Kirk, R. G., Guo, Z. and Balbahadur, A. C., "Synchronous Thermal Instability Prediction for Overhung Rotors," Proc. 22nd Texas A&M Turbomachinery Symp., Sept. 2003.

The authors can be contacted at: bill.marscher@mechsol.com.